New high temperature gas nitriding cycle that enhances the wear resistance of duplex stainless steels

C. M. GARZÓN, A. P. TSCHIPTSCHIN*
Metallurgical and Materials Engineering Department, University of São Paulo, Av. Prof. Mello Moraes 2463, CEP 05508-900, São Paulo, Brazil
E-mail: antschip@usp.br

Interstitially dissolved nitrogen improves the corrosion and wear resistance as well as the mechanical properties of stainless steels (SS) [1–5]. Production routes of High Nitrogen Stainless Steels (HNSS) by alloying, pressure metallurgy, powder metallurgy, and solid-state diffusion have been studied [6–10]. In the production route, which involves solid-state diffusion, the steel surface and near surface regions are alloyed with nitrogen through chemical, implantation, plasma, or laser techniques [9, 10]. Recently, a chemical solid-state nitrogen alloying technique was developed [10–14], consisting in annealing SS in a N_2-containing gas atmosphere in the range 1273–1473 K. In this High Temperature Gas Nitriding treatment (HTGN), atomic nitrogen is absorbed at the surface of the steel and then diffuses into the near surface region. Case-depths from 0.5 to 2.0 mm and nitrogen contents in solid solution at the surface from 0.5–1.0 wt% can be obtained after 18 to 45 ks heat-treatments.

HTGN has been successfully used to improve the surface properties of martensitic, austenitic, ferritic-austenitic and martensitic-ferritic SS [7, 10–13, 15]. Particularly, when ferritic-austenitic duplex stainless steels (DSS) are nitrided austenitic cases of higher wear and corrosion resistances are formed, on high strength DSS ferritic-austenitic cores. Due to both high temperatures and long nitriding times: (i) the austenitic cases grow forming coarse columnar grains [10–13], and (ii) the maximum attainable nitrogen content in precipitate-free cases corresponds to the nitrogen solubility limit at that temperature. The solubility limit in austenite, relative to nitride precipitation, increases with temperature; however the amount of ferrite in the dual-phase non-nitrided core increases with temperature too. Thus the optimum nitriding temperature for DSS is between 1423 and 1448 K.

In the present work, a novel nitriding cycle that avoids formation of coarse grains in the austenitic case, inhibits nitride precipitation and leads to sharp textures is proposed. It consists on cycling the specimen between two different N_2 partial pressures, PN_2, (Fig. 1): a high-pressure stage (sorption stage) and a vacuum one (desorption stage). The high nitrogen pressure stage is a long term one where nitrogen is introduced in the specimen. It is followed by a short vacuum period ($PN_2 \sim 0$) where nitrogen desorption occurs and ferrite grains precipitate at the surface and in the near surface region of the specimen.

The transformation sequence at the surface during the conventional isobaric treatment and the new cyclical HTGN treatment can be understood using the two temperature versus nitrogen partial pressure diagrams shown in Fig. 2, which represent the gas-metal equilibrium for an UNS S31803 DSS. These diagrams were constructed using the CALPHAD (Computer Coupling of Phase Diagrams and Thermochemistry) method and Thermocalc® [16] with the TCFE database. The first one (Fig. 2a) is a stable equilibrium diagram, which is representative of nitriding treatments where PN_2 is not high enough to induce nitride precipitation, as well as nitriding treatments where PN_2 is high enough to induce nitride precipitation and the nitriding time is long enough to allow the completion of this precipitation. The other diagram (Fig. 2b) is a metastable equilibrium diagram, in which the M_2N precipitation was suppressed. The construction of this second diagram arises from experimental observations made in a previous work [14], where it was pointed out that the kinetics of the nitride precipitation reaction during HTGN of stainless steels is much more slower than the kinetics of nitrogen sorption in austenite. Thus, in the earliest stages of the nitriding treatment, where PN_2 is high enough to induce nitride precipitation, the equilibrium between the metal surface and the gas atmosphere is established without starting the nitride precipitation, which should occur at later stages. Therefore, the diagram in Fig. 2 is representative of the metastable gas-metal equilibrium conditions, established during short-term nitriding treatments, where PN_2 is high enough to induce nitride precipitation.

In the cyclical nitriding treatment an austenitic surface layer is formed during the first sorption stage (spot S-S in Fig. 2b). In this stage, PN_2 is greater than the one corresponding to the nitrogen solubility limit (spot I-T in Fig. 2a), however the time is not long enough to allow nitride precipitation. This pressure-supersaturation aims to maximize nitrogen absorption. This stage is followed by a desorption period, where ferrite precipitation at the surface and in the near surface region occurs (spot D-S in Fig. 2b), due to formation of a narrow denitrided near surface layer. Next, sorption and desorption stages are alternated. Cycling leads to ferrite

*Author to whom all correspondence should be addressed.

0022–2461

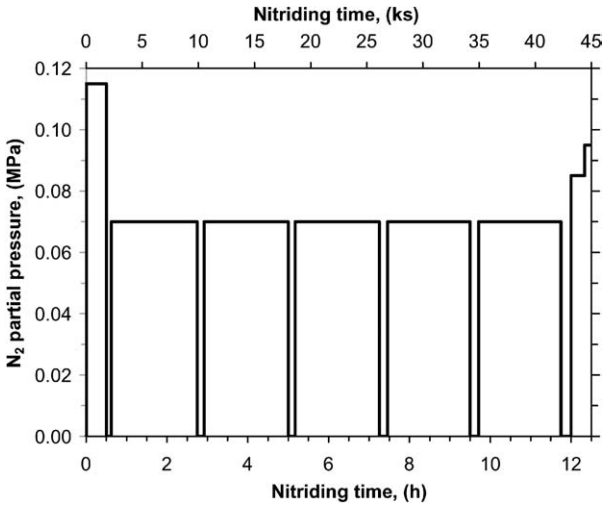

Figure 1 Nitrogen partial pressure as a function of nitriding time for the cyclic nitriding treatment.

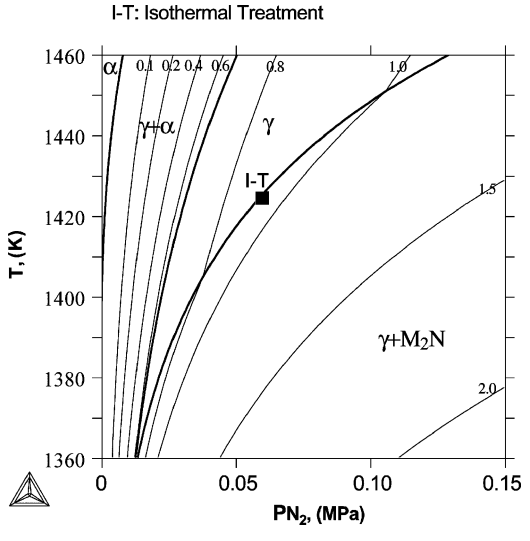

(a)

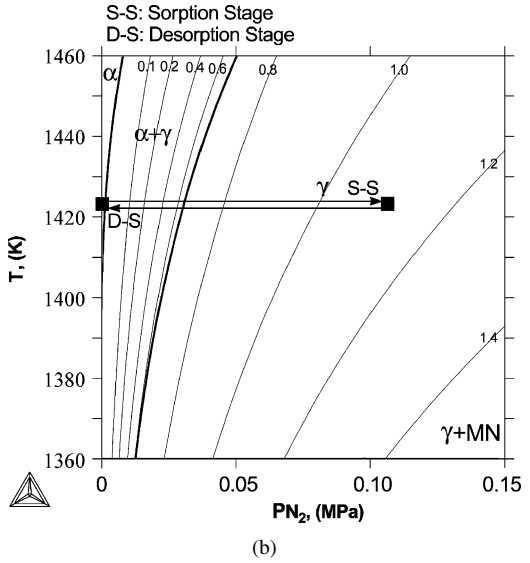

(b)

Figure 2 Temperature versus nitrogen partial pressure diagrams showing, phase fields (thick lines), surface nitrogen contents corresponding to gas-metal equilibrium (thin lines) and different HTGN treatment conditions (black squares): (a) Stable equilibrium diagram, and (b) metastable equilibrium diagram, in which M_2N precipitation was avoid.

TABLE I Chemical composition of UNS S31803 duplex SS and UNS S30403 austenitic SS (wt%)

Material	Cr	Ni	Mn	Mo	C	Cu	N	S	Si
S31803	22.5	5.4	1.9	3.0	0.019	0.14	0.16	<0.001	–
S30403	18.7	9.6	1.9	–	0.03	–	–	0.023	0.942

precipitation and re-dissolution, γ to $(\gamma+\alpha)$ and back to γ (Fig. 2b), inhibiting austenitic grain growth. In the intermediate sorption stages, PN_2 is slightly greater than the one corresponding to the nitrogen solubility limit, but it cannot be as high as in the first sorption stage because nitride precipitation should occur. To guarantee case thickening, several (between 3 and 7) intermediate sorption stages must be performed. The last sorption stage is a short one in which PN_2 is greater than the one corresponding to the nitrogen solubility limit (spot S-S in Fig. 2b) and it aims to maximize the nitrogen content at the surface of the samples.

Aiming to compare the microstructure and the surface properties of a DSS nitrided with the new cyclical treatment and with the conventional isobaric one, an UNS S31803 DSS was HTGN treated. Table I gives the chemical composition of the steel. The samples were heated up to 1423 K in a vacuum chamber, and then nitrided for 45 ks. The isobaric treatments were carried out under 0.06 MPa PN_2, which was the maximum nitriding pressure to obtain precipitate-free cases. The cyclic nitriding treatments were carried out following the nitriding scheme in Fig. 1.

After nitriding, an investigation of the microstructure, microtexture, hardness, nitrogen content, cavitation-erosion (CE), wear resistance, and pitting corrosion resistance of the UNS S31803 DSS samples was carried out. UNS S30403 austenitic SS samples were solution treated at 1423 K to use as comparison material in the CE wear tests. Table I gives the chemical composition of the S30403 SS.

The microtexture was determined by using electron back scattering diffraction (EBSD) coupled to a scanning electron microscope. The nitrogen content of the austenitic cases was determined by wavelength dispersive spectroscopy (WDS). The CE resistance was evaluated through vibratory CE experiments. The CE tests were carried out according to ASTM G32-92 standard, although a slight modification was introduced, using an indirect test arrangement. It consists of placing the test specimen below the vibrating horn. The separation between the samples and the vibrating horn was 0.5 mm. The vibratory frequency was 20 kHz and the peak to peak amplitude was 40 μm. The test medium was substitute ocean water at 293 K, prepared according to ASTM D 1141-90 standard. The pitting corrosion resistance was evaluated by potentiodynamic polarization experiments. The tests were carried out at 323 K in a solution with 5.0 % NaCl + 0.5M H_2SO_4, using a potential scanning rate of 600 mV/h.

Fig. 3 shows EBSD grain maps of the transverse section of the nitrided samples. Table II gives the times random (TR) intensity of the major texture components at the surface of the austenitic cases, as well as the mean grain diameter at both the surface and the

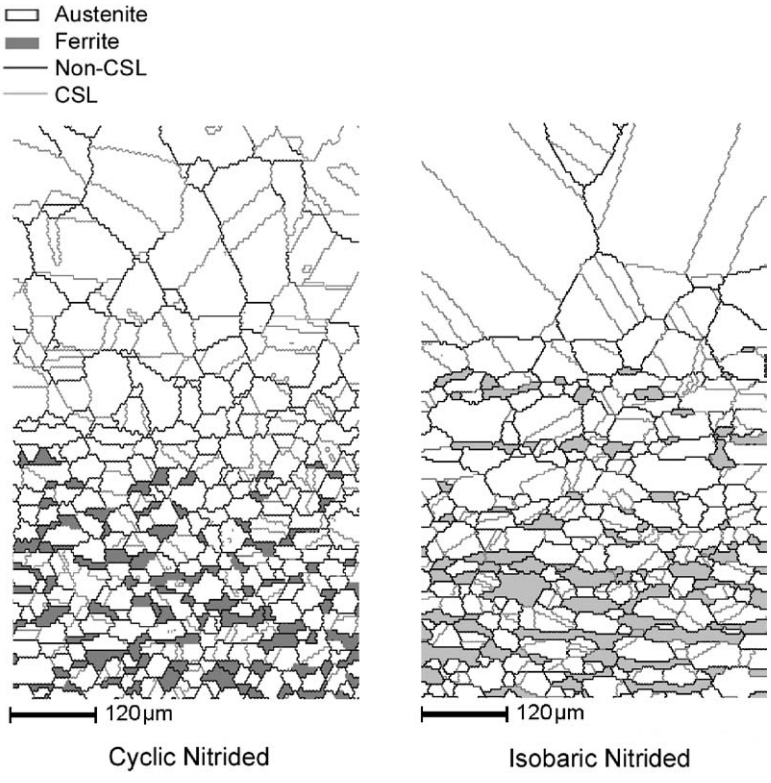

Figure 3 EBSD grain maps of the UNS S31803 DSS nitrided samples: (a) Isobaric nitriding treatment and (b) cyclic nitriding treatment.

TABLE II Mean grain diameter and texture intensity of the austenitic cases

Nitriding treatment	Mean grain diameter (μm)		Texture intensity (times random)	
	Surface	Transverse section	{100}⟨001⟩	{110}⟨112⟩
Cyclical	45	35	12	5
Isobaric	105	68	2	2

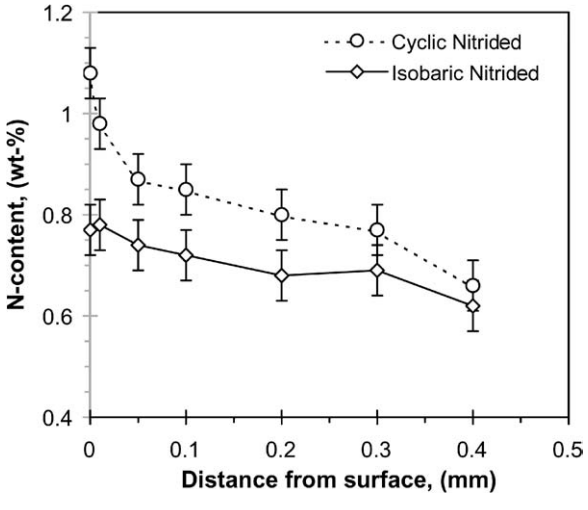

Figure 4 WDS measured nitrogen content in the austenitic case as a function of depth beneath the surface.

transverse section of the cases. In Fig. 3, from the surface to the core of the samples, two different regions can be observed: a fully austenitic surface layer (ASL) and a dual-phase region (DPR), composed by a layered austenite-ferritic microstructure. With regard to the conventional isobaric nitriding treatment, the microstructure and the microtexture of the cyclic nitrided samples display three distinct features: the grains are smaller, the columnar structure is avoided and the texture is sharper.

Fig. 4 shows WDS-measured nitrogen contents in the austenitic cases, from the surface inwards. The cyclical nitriding treatment leads to greater nitrogen contents in the surface, as well as in the near surface region. This is due to the pressure-supersaturation achieved during the sorption stages. As a consequence of the greater nitrogen content and the finer microstructure obtained in the cyclical treated specimens, Vickers hardness was greater in the cyclical treated specimens too. Vickers hardness tests, varying the testing load between 0.01 e 10 kgf, were carried out on top of the nitrided samples. Fig. 5 shows the results of those measurements. The new cyclical nitriding treatment leads to austenitic cases with both higher micro hardness and macro hardness, which guarantees a better surface load-bearing capacity.

Fig. 6 shows the potentiodynamic polarization curves obtained in the corrosion tests. No significant changes in pitting potential (∼875 mV ECS) were observed.

Fig. 7 shows the cumulative mass loss as a function of CE exposure time. The curves can be divided into two stages, namely, an incubation period, where the mass loss is very small, and a damage period, where the cumulative mass loss increases with exposure time. Moreover, in the damage period the mass loss rate increases with exposure time, tending to a stationary value, i.e., the maximum mass loss rate. The samples cyclically nitrided presented a maximum mass loss rate 3.2 times lower than the isobaric treated ones, and an incubation

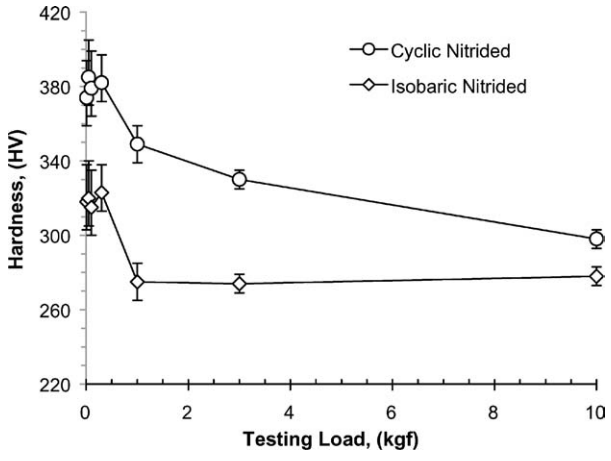

Figure 5 Vickers hardness on top of the samples as a function of testing load.

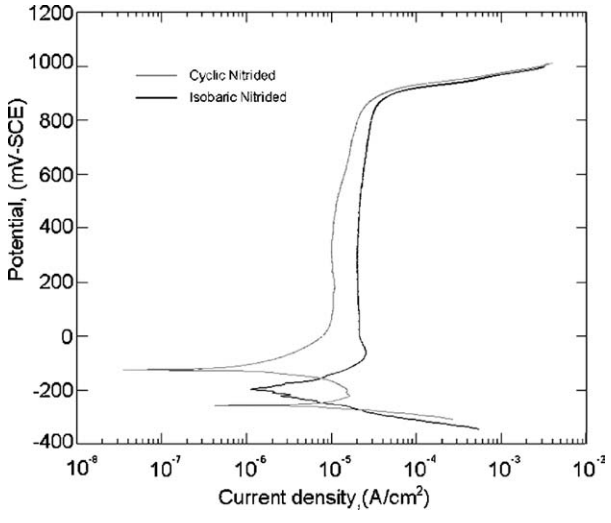

Figure 6 Potentiodynamic polarization curves.

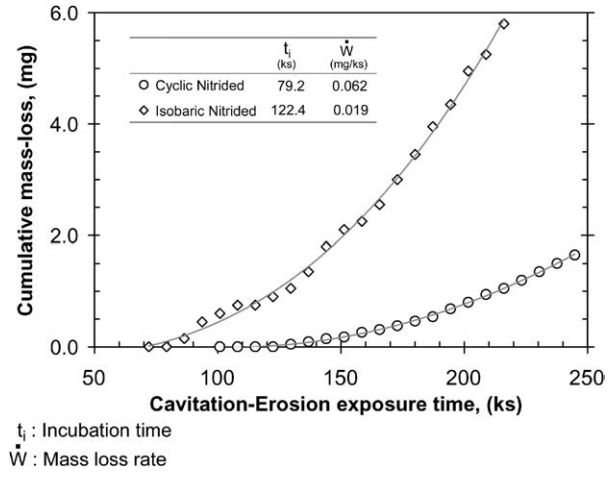

Figure 7 Cumulative mass loss as a function of CE exposure time.

period 1.6 higher. The better wear resistance observed in the cyclically nitrided samples can be explained, in part, by the synergetic hardening interaction between grain refinement and nitrogen alloying, which was recently proposed to HNSS [19]. However, it should be noted that the hardness increase (Fig. 6) is not proportionally intense as the decrease in CE mass loss rate

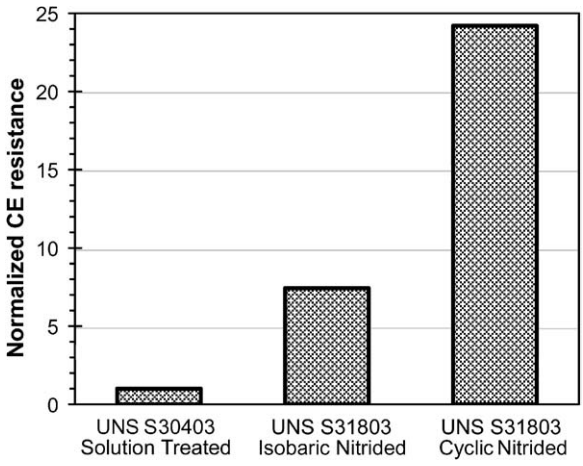

Figure 8 Normalized CE resistance of the samples.

(Fig. 7). Thus, the observed decrease in CE mass loss rate cannot be related just to hardening, and a beneficial effect of microtexture should also be taken into account.

Fig. 8 shows the ratio between the mass-loss rate of the UNS S30403 SS solution treated samples and the mass-loss rate of the S31803 nitrided samples, i.e., the normalized CE resistance. One can see that the cyclic nitrided samples are 24.2 more resistant than the S30403 SS solution treated samples. It is also worth noting that the normalized CE resistance of the cyclically nitrided samples is similar to the normalized CE resistance of the more expensive CE resistant Co-based alloys, which ranges between 3 and 32 [20].

Acknowledgment

The authors acknowledge the financial support of the Fundação de Amparo à Pesquisa do Estado de São Paulo (FAPESP), Brazil.

References

1. V. G. GAVRILJUK, *ISIJ International* **36** (1996) 738.
2. H. HÄNNINEN, J. ROMU, R. ILOLA, J. TERVO and A. LAITINEN, *J. Mater. Proc. Tech.* **117** (2001) 424.
3. J. TERVO, *Mater. Sci. Forum* **318–320** (1999) 743.
4. H. HÄNNINEN, *ibid.* **318–320** (1999) 479.
5. A. P. TSCHIPTSCHIN and A. TORO, "HNS 2003—High Nitrogen Steels" (vdf Hochschulverlag, Zurich, 2003) p. 229.
6. H. BERNS, *ISIJ International* **36** (1996) 909.
7. V. G. GAVRILJUK and H. BERNS, "High Nitrogen Steels" (Springer-Verlag, Berlin, 1999) p. 378.
8. A. TORO, N. ALONSO-FALLEIROS, D. RODRIGUES, F. AMBROSIO FILHO and A. P. TSCHIPTSCHIN, *Trans. Indian Inst. Met.* **55** (2002) 481.
9. U. KAMACHI, H. S. KHATAK, R. BALDEV and M. UHLEMANN, "HNS 2003—High Nitrogen Steels" (vdf Hochschulverlag, Zurich, 2003) p. 229.
10. H. BERNS and S. SIEBERT, *ISIJ International* **36** (1996) 927.
11. H. BERNS, German Patent, DE4033706 (1991).
12. H. BERNS, R. L. JUSE, J. W. BOUWMAN and B. EDENHOFER, *Heat Treat. Met.* (2000) 39.
13. H. BERNS, U. EUL, E. HEITZ and R. JUSE, *Mater. Sci. Forum* **318–320** (1999) 517.
14. C. M. GARZÓN, A. TORO and A. P. TSCHIPTSCHIN, *Trans. Indian Inst. Met.* **55** (2002) 255.

15. A. TORO, W. MISIOLEK and A. P. TSCHIPTSCHIN, *Acta Mater.* **51** (2003) 3363.
16. J.-O. ANDERSSON, T. HELANDER, L. HÖGLUND, P. SHI and B. SUNDMAND, *Calphad* **26** (2002) 273.
17. A. DI SCHINO and J. M. KENNY, *J. Mater. Sci. Lett.* **21** (2002) 96.
18. A. DI SCHINO, M. BARTERI and J. M. KENNY, *J. Mater. Sci.* **38** (2003) 3257.
19. M. O. SPEIDEL, "HNS 2003—High Nitrogen Steels" (vdf Hochschulverlag, Zurich, 2003) p. 229.
20. J. H. BOY, A. KUMAR, P. MARCH, P. WILLIS and H. HERMAN, Usacerl Technical Report 97/118 (Usacerl, USA, 1997) p. 144.

Received 7 May
and accepted 23 June 2004